Supplementary Material for

Succination inactivates gasdermin D and blocks pyroptosis

Fiachra Humphries, Liraz Shmuel-Galia, Natalia Ketelut-Carneiro, Sheng Li, Bingwei Wang, Venkatesh V. Nemmara, Ruth Wilson, Zhaozhao Jiang, Farnaz Khalighinejad, Khaja Muneeruddin, Scott A. Shaffer, Ranjan Dutta, Carolina Ionete, Scott Pesiridis, Shuo Yang, Paul R. Thompson, Katherine A. Fitzgerald*

*Corresponding author. Email: kate.fitzgerald@umassmed.edu

Published 20 August 2020 as *Science* First Release
DOI: 10.1126/science.abb9818

This PDF file includes:

Other Supplementary Material for this manuscript includes the following:
(available at science.sciencemag.org/content/science.abb9818/DC1)

Materials and methods

Mice

All animal experiments were approved by the Institutional Animal Care Use Committees at the University of Massachusetts Medical School. Animal were kept in specific pathogen free (SPF) environment. Male and female C57/BL6 and *Gsdmd*$^{-/-}$ mice were used. *Gsdmd*$^{-/-}$ mice were generated as previously described (*22*). *Mefv*$^{V726/V726}$ mice were a gift from Prof. Daniel Kastner (*23*). Sample sizes used are in line with other similar published studies. All animals were used at age 4-12 weeks.

Reagents

All chemicals and metabolites were purchased from sigma. Metabolites were dissolved in DMSO and used at the follow concentrations based on previous published studies *(7, 8 ,9)*: alpha-ketoglutarate (1 mM), succinate (5 mM), methyl/ethyl pyruvate (5 mM), diethyl butyl malonate (1 mM), dimethyl fumarate (25 μM), monomethyl fumarate (25 μM), 4-octyl itaconate (50 μM) triethyl citrate (10mM). Nigericin (N7143) was purchased from sigma. LPS (ALX-581-010-L002) was from enzo. Cells were transfected using genejuice according to the manufacturer's instructions.

Plasmids

All GSDMD constructs were purchased from addgene. Full length FLAG-GSDMD (#80950), FLAG-GSDMD-NT (#80951), FLAG-GSDMD-NT-C192A (#133891).

Cell Culture

Human kidney cell line HEK293T were cultured in Dulbecco's modified Eagle's medium supplemented with 10% (v/v) fetal bovine serum, 100U/ml penicillin and 100μg/ml streptomycin. Human peripheral blood monocyte cell line, THP1 cells were cultured in RPMI-1640 medium supplemented with 10% (v/v) fetal bovine serum, 100 U/ml penicillin and 100 μg/ml streptomycin. For isolation of BMDMs, tibias and femurs were removed from wild type and *Gsdmd*$^{-/-}$ mice and bone marrow was flushed with complete DMEM-medium. Cells were plated in medium containing 20% (v/v) conditioned medium

of L929 mouse fibroblasts cultured for 7 days at 37°C in a humidified atmosphere of 5% CO_2. Medium was replaced every 3 days.

ELISA

Conditioned media or serum was collected as indicated and mouse IL-1β or TNF-α, were quantified by sandwich ELISA (R&D Systems).

Cell death assays

Cells were plated, treated and incubated in phenol red-free medium. Following treatment, medium was collected and assessed for LDH release using the CytoTox96 non-radioactive cytotoxicity assay (Promega) as per manufacturer's instructions. Kinetic cell death assays were performed using SYTOX Orange and the Biotek Cytation5.

Inflammasome activation assays

Cells were primed with LPS (100 ng/ml) from *Escherichia coli* serotype EH100 (ra) TLRgrade for 3 hours followed by stimulation with the inflammasome activator nigericin (10 μM) for 1 hour. For noncanonical inflammasome activation, cells were primed with l μg/ml Pam3CSK4 (Invivogen) for 2 hours, followed by transfection of LPS (2 μg/ml) using Lipofectamine 2000 for 16 hours. Salmonella infection and poly dA:dT transfection was performed as previously described (*22*). For salmonella infections strain *Salmonella enterica* serovar Typhimurium SL1344 (*S.* Typhimurium) was grown to log phase and infected at a MOI of 10.

Immunoblotting and Immunoprecipitation

Primary BMDMs from WT or *GsdmD*$^{-/-}$ mice were cultured in 12-well plates (1×10^6 cells per ml; 1 ml) or 10-cm dishes (2×10^6 cells per ml; 10ml). HEK293T cells (2.5×10^5 cells per ml; 3 ml) were cultured in 6-well plates and transfected with FLAG-tagged GSDMD constructs where indicated. For cell lysate analysis cells were lysed directly in 1X Lamelli sample buffer. For native gel analysis cells were lysed in in NP-40 lysis buffer (50 mM Tris-HCl, pH 7.4, containing 150 mM NaCl, 0.5% (w/v) IgePal, 50 mM NaF, 1 mM Na3VO4, 1 mM dithiothreitol, 1 mM phenylmethylsulfonyl fluoride and protease

inhibitor cocktail. For immunoprecipitation of GSDMD, cells were treated as indicated and then collected in 500 µl RIPA buffer, followed by incubation for 15 min on ice. Lysates were incubated with GSDMD antibody and protein A–protein G-agarose was added to each sample, followed by incubation overnight at 4°C. Immunoprecipitates were collected by centrifugation and washed four times with 1 ml of RIPA buffer. Immunprecipates were eluted from beads using 1X sample buffer. Samples were resolved by SDS-PAGE and stained using simply blue safe stain or transferred to nitrocellulose membranes and analyzed by immunoblot. Immunoreactivity was visualized by the Odyssey Imaging System (LICOR Biosciences). For immunoblotting of IL-1β in cell supernatants, conditioned medium was collected and filtered using filter spin columns to reduce salt and remove abundant serum proteins. Filtrates were added to 4X SDS-PAGE sample buffer and resolved by SDS-PAGE for immunoblot analysis. GSDMD (ab209845) and GSDME antibodies were from abcam (ab215191). Caspase 1 antibody was from adipogen. Fumarase antibody was from cell signalling and anti-β-actin (AC-15; A1978) were from Sigma; anti-mouse IRDyeTM 680 (926-68070) and anti-rabbit IRDyeTM 800 (926-32211) were from LI-COR Biosciences

Intact protein analysis

Intact mass analysis of GSDMD protein was carried out using an Acquity UPLC (Waters Corporation, Milford, MA) coupled to a Synapt G2-Si (Waters) quadrupole time-of-flight mass spectrometer fitted with an electrospray ionization source. Liquid chromatography was carried out with a 3.0 x 50 mm(4µm) MAbPac RP column (Thermo Scientific, Waltham, MA) using mobile phase A and B containing 0.1% (v/v) formic acid in water, and 0.1% (v/v) formic acid in acetonitrile, respectively. A total of 0.6 µg sample was injected and the protein eluted using a linear gradient of 10 to 70% B over 7.0 minutes at a flow rate of 0.3 ml/min. Mass spectrometry detection using Synapt G2-*Si* was acquired in positive mode from *m/z* 100–2000 and the conditions were optimized as follows: sampling cone, 120 V; source offset, 100 V; source temperature, 90 °C ; desolvation temperature, 120 °C; cone gas flow,50 L/h; desolvation gas flow, 600 L/h. Calibration was performed using Glu-1-Fibrinopeptide B. Deconvolution of raw mass spectrum was performed with MaxEnt 3.1 (Waters) software.

Peptide mapping by nano LC-MS/MS

Cell lysates were run by SDS gel electrophoresis and bands for GSDMD were excised, pooled and subjected to in-gel digestion with trypsin. The resulting peptides were lyophilized, re-suspended in 5% acetonitrile, 0.1% (v/v) formic acid in water and injected onto a NanoAcquity UPLC (Waters) coupled to a Q Exactive (Thermo Scientific) hybrid quadrapole orbitrap mass spectrometer. Peptides were trapped on a 100 µm I.D. fused-silica pre-column packed with 2 cm of 5 µm (200Å) Magic C18AQ (Bruker-Michrom) particles in 5% acetonitrile, 0.1% (v/v) formic acid in water at 4.0 µl/min for 4.0 minutes. Peptides were then separated over a 75 µm I.D. gravity-pulled 25 cm long analytical column packed with 3 µm (100Å) Magic C18AQ particles, at a flow rate of 300 nl/min containing mobile phase A, 0.1% (v/v) formic acid in water and mobile phase B, 0.1% (v/v) formic acid in acetonitrile, using a biphasic gradient: 0-60 min (5-35% B), 60-90 min (35-60% B), 90-93 min (60% B), 93-94 min (60-90% B), 94-109 (90% B), followed by equilibration to 5% B. Nano-ESI source was operated at 1.4 kV via liquid junction. Mass spectra were acquired over *m/z* 300-1750 at 70,000 resolution (*m/z* 200) with an AGC target of 1e6. Data-dependent acquisition (DDA) selected the top 10 most abundant precursor ions for tandem mass spectrometry by HCD fragmentation using an isolation width of 1.6 Da, max fill time of 110ms, and AGC target of 1e5. Peptides were fragmented by a normalized collisional energy of 27, and product ion spectra were acquired at a resolution of 17,500 (*m/z* 200). Raw data files were peak processed with Proteome Discoverer (version 2.1, Thermo Scientific) followed by identification using Mascot Server (Matrix Science) against the *Mouse* (Swissprot) FASTA file (downloaded 07/2019). Search parameters included full tryptic enzyme specificity, and variable modifications of N-terminal protein acetylation, oxidized methionine, glutamine conversion to glutamic acid, 2-dimethyl succinylation, 2-monomethyl succinylation, 2-succination, and carbamidomethylation on cysteine. Assignments were made using a 10 ppm mass tolerance for the precursor and 0.05 Da mass tolerance for the fragment ions. All non-filtered search results were processed by Scaffold (version 4.8.4, Proteome Software, Portland, OR) utilizing the Trans-Proteomic Pipeline (Institute for Systems Biology, Seattle, WA) at 1% false-discovery rate (FDR) for peptides and 99% threshold for proteins (2 peptides minimum).

Metabolite extraction and quantification

$5x10^7$ cells in serum free medium were placed on ice and medium and cells were thoroughly scraped in 5 mL of 80% methanol solution and transferred to a 15ml tube. Cells were then vortexed for 10 min at 4°C. Cell lysates were then centrifuged at 13,000 g for 10 min. Supernatant was collected and stored at -80°C until processing for LC/MS. Samples were spiked with 2 µl of 7.5µM ^{13}C4 fumaric acid (Cambridge Isotope Laboratories, Tewksbury, MA) and dried in a SpeedVac. Proteins were precipitated with 200 µl of ice-cold 95% acetonitrile, 5% water (0.05% (v/v) formic acid), and the supernatant separated and dried by SpeedVac. The resulting residue was reconstituted in 50 µl of 95% acetonitrile, 5% water (0.05% formic acid) for liquid chromatography–tandem mass spectrometry (LC-MS/MS). For analysis, 5 µl aliquots were injected in technical triplicate onto a 2.1 x 150 mm (1.7µm) BEH Amide (Waters) column using an Acquity UPLC (Waters) coupled to a Xevo TQ-XS (Waters) triple quadrupole mass spectrometer operating in the negative ion electrospray mode. The flow rate was 0.2 ml/min and mobile phase A (0.05% formic acid in water) and B (0.05% formic acid in acetonitrile) were used to elute fumarate using the following gradient conditions: 0-2 min (95% B), 2-8.2 min (95%-60% B), 8.2-8.5 min (60%-40% B), 8.5-9.5 min (40-95%B), and 9.5-13 min (95%B). Data was collected using selected reaction monitoring for fumarate and labeled internal standard using *m/z* 114.9>71 and 119>74 mass transitions, respectively. A calibration curve was constructed in a lysate free solution of 95% acetonitrile, 0.05% formic acid in water. Two-fold serial dilutions were carried out using a working solution of 400 µM fumaric acid to obtain 12 points across the range of 0.08 - 400 µM, each spiked with 0.3 µM of ^{13}C4 fumarate and were injected in technical duplicates. Peak areas were integrated in TargetLynx XS (Waters) and data analysis was carried out in Excel (Microsoft, Redmond, WA) and Prism (GraphPad Software, San Diego, CA). Sample concentrations were determined from the calibration curve (fitted with 1/X weight factor and $R^2 = 0.998$). The relative standard deviations (RSDs) for the triplicate analyses were all within 10%.

siRNA gene knockdown

WT BMDMs were transfected with control non-targeting siRNA or NRF2 specific siRNA (50nM) for 48 hours and assayed as indicated. siRNA 1 Thermofisher, 4390815/Assay ID: s70521, siRNA 2 Thermofisher 4390815/Assay ID: s70523.

LPS septic shock model

Mice aged 8-12 weeks were administered LPS (*E. coli* 0111: B4, Sigma) 5 mg/kg by intraperitoneal injection. Serum was collected after 5 hours for ELISA analysis. For survival studies, mice were administered 50 mg/kg of LPS intraperitoneally and monitored every 12 hours for up to 96 hours.

In vitro succination reaction

1 μg of purified human or murine GSDMD was incubated with 25 μM of DMF or MMF in 50μl of incubation buffer (250 mM HEPES, 2 mM EDTA and 0.1 mM neocuproine) and incubated for 3 hours at 37°C.

In vitro binding assay

HEK293T cells were transfected with 1 μg of caspase 1 and immunoprecipitated on protein A/G beads. gasdermin-d was pre-succinated in vitro as above and incubated with caspase 1 protein A/G beads. Caspase 1 beads were incubated with or without native recombinant GSDMD in 1ml of lysis buffer rotating for 6 hours at 4°C overnight.

Induction and assessment of EAE

Mycobaterium tuberculosis H37Ra (231141) was from BD. Incomplete Freund's adjuvant (F5506) was from Sigma-Aldrich. MOG35-55 peptide (residues 35–55, Met-Glu-Val-Gly-Trp-Tyr-Arg-Ser-Pro-Phe-Ser-Arg-Val-Val-His-Leu- Tyr-Arg-Asn-Gly-Lys) was synthesized by Sangon Biotech. EAE was induced using MOG_{35-55} peptide (200 μg per mouse) emulsified with CFA (50 μl per mouse, including 4 mg/ml *M. tuberculosis* H37Ra) and 50 μl of incomplete Freund's adjuvant. 250 ng of Pertussis toxin was administered IV on day 0 and 2 post immunization. Mice were scored daily for clinical signs of EAE in a blinded fashion. EAE score was calculated as follows: 0.5, partial tail paralysis; 1, tail paralysis; 1.5, reversible corrective reflex impairment; 2,

corrective reflex impairment; 2.5, one hindlimb paralysis; 3, both hindlimbs paralysis; 3.5, both hindlimbs paralysis and one forelimb paralysis; 4, hindlimb and forelimb paralysis; and 5, death.

Histological and immunohistochemistry

Tissue blocks were sectioned at 5 μm thick. For paraffin-embedded tissue, CNS tissue was rapidly dissected from mice perfused with PBS. Tissues were fixed in 4% paraformaldehyde overnight. Tissue sections were stained with H&E for evaluation of inflammation. IHC staining of GSDMD was performed with anti-GSDMD antibody (Abcam, ab219800) and detected using horseradish peroxidase-conjugated secondary antibodies after heat-induced antigen retrieval as previously described (*18*). Diaminobenzidine was used for detection. Images were captured with a Nikon Ds-Ri2 microscope. Histological scores: 0, no inflammatory cell infiltration and no demyelination; 1, slight inflammatory cell infiltration or demyelination observed; 2, moderate inflammatory cell infiltration or demyelination in several spots; 3, substantial inflammatory cell infiltration and large area of demyelination.

DMF mouse diet

DMF embedded mouse diet was formulated by Lab Diets®. DMF was added to a base diet of laboratory lab diet 5001 at a dose 100mg/kg/day of consumption. Mice received the control base diet or the DMF containing diet for 6 weeks.

Human Brain Autopsies

Post-mortem lesions were collected from PMS patients (Table S4) as previously described (*24*). Briefly, tissue blocks fixed in 4% paraformaldehyde were 30 μM sections were fixed on superfrost slides and stained for GSDMD-N p30 (Cell signalling, 36425s) as previously described. IHC staining was performed by applied pathology systems, Shrewsbury, MA.

Flow cytometry

For analysis of infiltrating immune cells CNS, brains, and spinal cords from $MOG_{35–55}$-immunized mice were excised and digested at 37°C with collagenase type IV (0.5 mg/ml; Sigma-Aldrich) and DNase I (10 U/ml; Roche) in RPMI 1640 under agitation (200 rpm) conditions for 1 hour. Following digestion, tissues were filtered through a 100-µm filter. Cell suspensions separated using a Percoll density gradient (GE Healthcare) and separated by collecting the interface fractions between 37% and 70% Percoll. Mononuclear cells were isolated from the interface. The cells were suspended in PBS containing 2% (wt/vol) FBS. Cells were washed three times and stained with cell surface marker antibodies for flow cytometric analysis. The following antibodies were used: Anti-CD45-FITC (30-F11,11-0451-82), anti-CD4-FITC (GK1.5, 11-0041-82), anti-CD8a-PE (53–6.7,12-0081-83), anti-CD11b-APC (M1/70,17-0112-82), anti-IL17A-PE (eBio17B7,12-7177-81), anti-IFN-γ-APC (XMG1.2,17-7311-81), Fixable Viability Dye eFluor™ 506 (65-0866-14), and Intracellular Fixation & Permeabilization Buffer Set Kit (85-88-8824-00) were from eBioscience. Anti-CD4-APC-Cy7 (GK1.5,100414) was from Biolegend. All flow cytometry was performed on an Attune NxT flow cytometer (Thermo Fisher Scientific), and data were analyzed by FlowJo 7.6.1 software.

Synthesis of methyl (*E*)-4-oxo-4-(propynylamino)-2-butenoate (MMF-alkyne, 1)

Propargylamine (0.141 ml, 2.2 mmol) and DIPEA (0.38 ml, 2.2 mmol) were added to a solution of monomethyl fumarate (0.25 g, 1.9 mmol) and HATU (0.76 g, 2.0 mmol) in dimethyl Formamide (5 ml) at ice cold condition. The reaction mixture was stirred at room temperature for 20 hours. The reaction mixture was poured into water to precipitate the crude compound. This crude mixture was dissolved in CH_3CN: H_2O (1:4) and purified by preparative HPLC (CH_3OH:CH_3CN) to yield the product **1** as a white solid (90%). ^1H NMR (500 MHz, DMSO) δ 9.1 (bs, 1H), 7.0 (d, J = 16.0 Hz, 1H), 6.7 (d, J = 16.0 Hz, 1H), 4.16 (dd, J = 5.3, 2.6 Hz, 2H), 3.80 (s, 3H), 3.2 (t, J = 2.6 Hz, 1H). ^{13}C NMR (DMSO) δ 166.08, 163.29, 135.76, 130.90, 78.80, 72.39, 52.45, 29.77. MS (ESI+): 168.2 ($M+H^+$). ^1H and ^{13}C NMR spectra were recorded in d_6-DMSO as solvent using a Bruker 500 MHz NMR spectrometer. Chemical shift values are cited with respect to TMS as the internal standard. Reverse-phase HPLC using a semi-preparative C18 column

(Agilent, 21.2×250 mm, 10 μm) and a water/acetonitrile gradient supplemented with 0.05% trifluoroacetic acid.

Copper click chemistry

Cells treated with or without the MMF-Alkyne probe were lysed and quantified by protein DC assay. Proteome samples (2 mg/ml) were incubated with TCEP, TBTA ligand, copper sulphate and Biotin Azide for 1 hour at room temperature with vortexing every 15 min. Precipitated proteins were centrifuged for 5 minutes at 4600*g*. Protein pellets were washed twice with ice cold methanol and sonicated in 1.2% SDS. Samples were heated at 95°C for 5 min and diluted to a final volume of 6 ml with PBS (0.2% SDS). An aliquot of the post-clicked lysate was retained and the remainder was incubated with streptavidin beads on a rotator overnight at 4°C. Samples were rotated at room temperature for 2 hours to resolubilize the SDS. Beads were washed five times with 0.2% SDS/PBS and placed on a rotator for 10 min in between washes. Beads were washed with ultra-pure water a further three times. At this point beads were eluted in 1X sample buffer or further processed for mass spec as described.

PBMC isolation

PBMC were isolated from whole blood of consenting donors. Blood was diluted 1:1 in sterile PBS and layered over 15 mls of Lymphoprep. Blood was spun at 450*g* with no break. The interphase was transferred to a fresh tube using a Pasteur pipette and washed twice in PBS. Red blood cells were lysed in red blood cell lysis buffer for 10 min at room temperature. Cells were washed once more in PBS and counted.

Ethics

All animal studies were performed in compliance with the federal regulations set forth in the Animal Welfare Act (AWA), the recommendations in the Guide for the Care and Use of Laboratory Animals of the National Institutes of Health, and the guidelines of the UMass Medical School Institutional Animal Use and Care Committee. All protocols used in this study were approved by the Institutional Animal Care and Use Committee at the UMass Medical School (protocols A-1633). All patient samples were donated following

informed consent under the approved IRB protocol “Family Studies in Demyelinating Disorders", IRB reference number: H-14143.

Statistical analysis

For comparisons of two groups two-tailed students’ t test was performed. Multiple comparison analysis was performed using two-way ANOVA. Mann-Whitney U test was used for EAE analysis. Mantel-Cox were used for survival analysis. Three to ten mice were used per experiment, sufficient to calculate statistical significance, and in line with similar studies published in the literature.

Figure S1

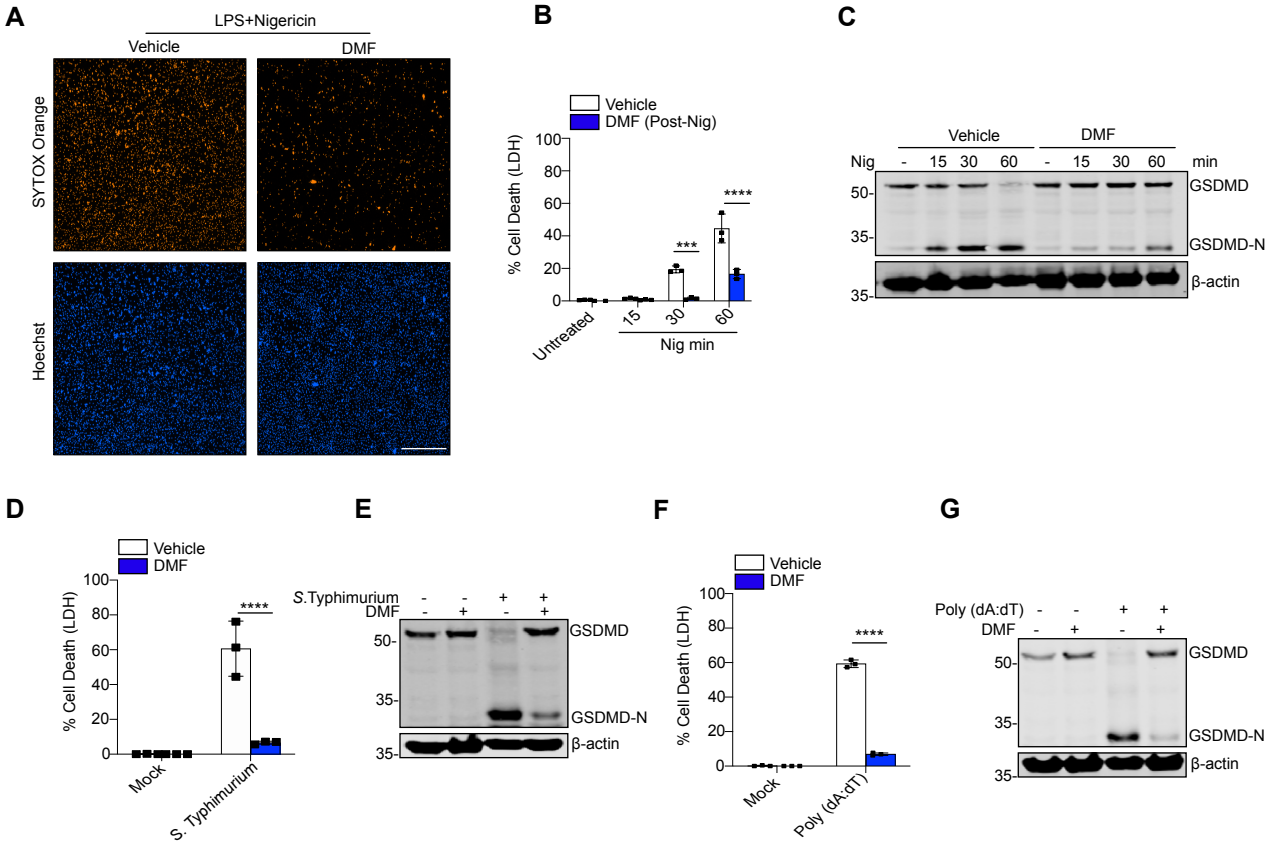

Fig. S1. Fumarate inhibits pyroptosis. **(A)** SYTOX Orange and Hoechst stained WT BMDMs treated with LPS for 2 hours, DMSO (vehicle) or DMF (25 μM) for 1 hour and nigericin for 6 hours, scale bar 500 μm. **(B)** LDH assay conditioned medium from WT BMDMs treated with LPS for 3 hours, nigericin for the indicated times and DMSO (vehicle) or DMF (25 μM) 15 minutes after each nigericin (10 μM) timepoint. **(C)** Immunoblot analysis of GSDMD in BMDMs treated as in (C). **(D-E)** LDH (D) and immunoblot analysis of GSDMD and β-actin in lysates (E) from WT BMDMs treated with DMSO (vehicle) or DMF (25 μM) for 1 hour followed by infection with strain Salmonella enterica serovar Typhimurium SL1344 (S.Typhimurium) at log phase (MOI=10). salmonella infection (MOI 10) for 6 hours. **(F-G)** LDH (F) and immunoblot analysis of GSDMD and β-actin in lysates (G) from WT BMDMs primed with LPS for 2 hours, followed by treatment with DMF (25 μM) transfection with Poly (dA:dT) (1 μg). A, C, E, G are representative of 3 independent experiments. B, D, F are pooled data from 3 independent experiments. ***,

Figure S2

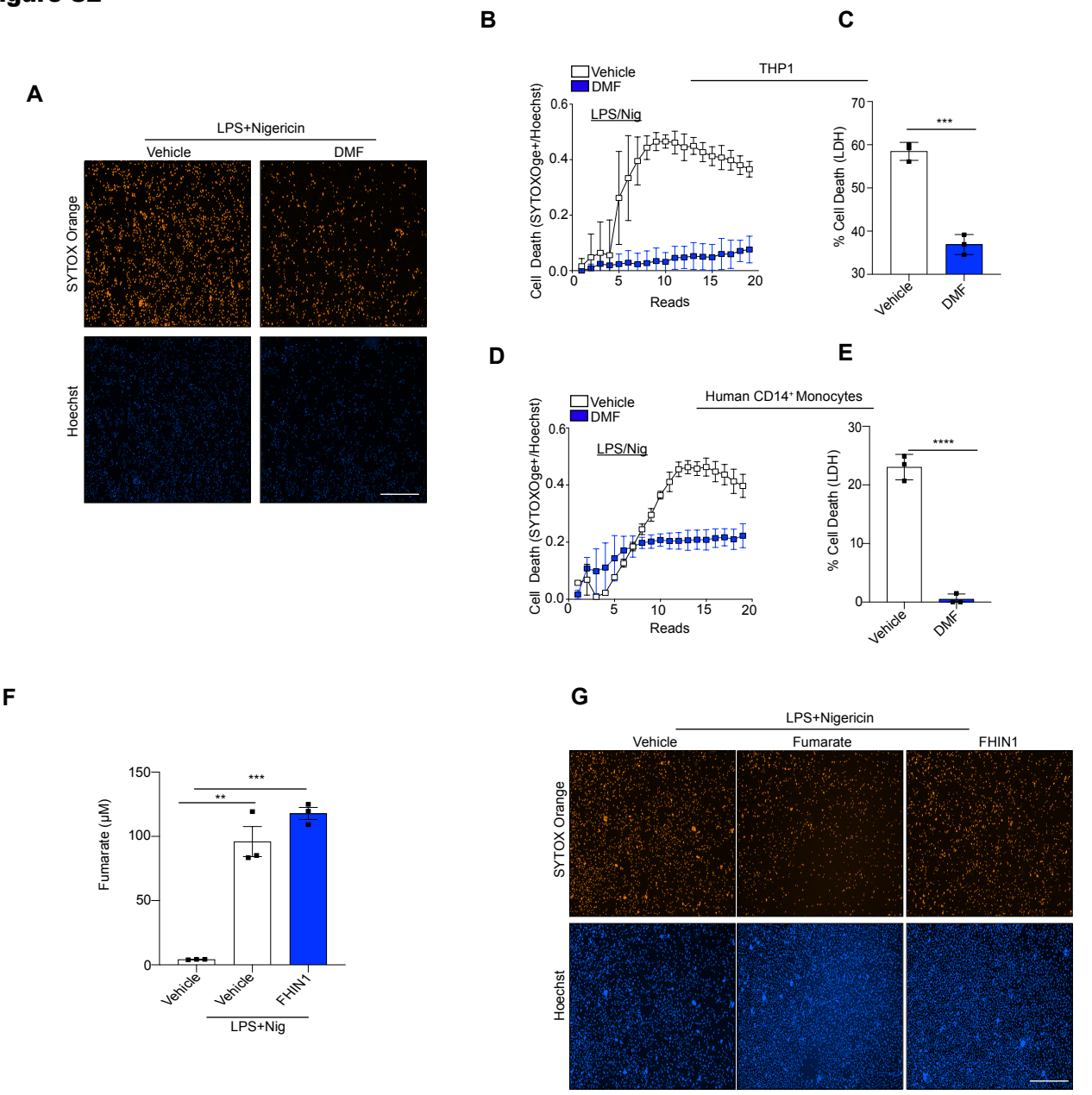

Fig. S2. Fumarate inhibits pyroptosis in Human cells. (**A-B)** Representative images (A) and kinetic data (B) of SYTOX Orange and Hoechst-stained PMA-differentiated THP1 cells treated with LPS for 2 hours, DMSO (vehicle) or DMF (25 μM) for 1 hour and nigericin (10 μM) for 6 hours. **(C)** LDH release from (A). **(D-E)** Kinetic cell death data of SYTOX Orange and Hoechst stained (D) or LDH assay of conditioned medium from primary $CD14^+$ positive monocytes treated with LPS for 2 hours DMSO (vehicle) or DMF (25 μM) for 1 hour and nigericin (10 μM) for 6 hours. **(F)** LC/MS quantification of DMF in WT BMDMs treated with LPS for 2 hours, FHIN1 for 1 hour and nigericin for 1 hour. **(G)** Representative images of WT primary BMDMs stained with SYTOX Orange and Hoechst following treatment with LPS for 2 hours, DMSO (vehicle) or DMF (25 μM) or FHIN1 (25 μM) for 1 hour and nigericin for a timecourse of 6 hours. A, B, D, G are representative of 3 independent experiments. C, E, F are pooled data from 3 independent experiments. ***, $P < 0.001$, ****, $P < 0.00001$ (Students t-test). Error bars show mean ± SD (B, D) or SEM (C, E). A, G scale bar, 500 μm.

Figure S3

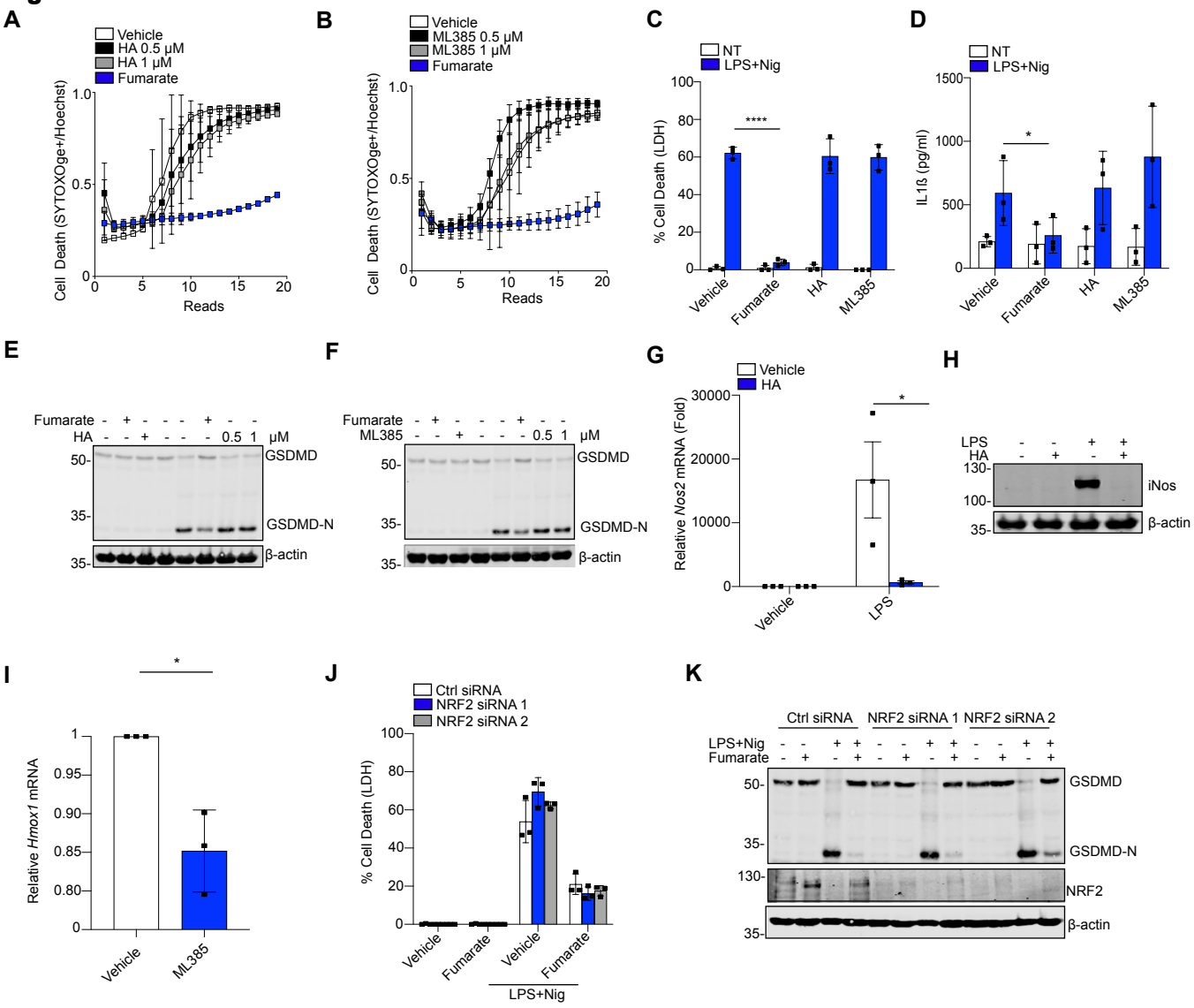

Fig. S3. Fumarate regulates pyroptosis independently of NRF2 and GAPDH. **(A-B)** Kinetic cell death data of WT primary BMDMs treated with LPS for 2 hours, DMSO (vehicle) or DMF (25 µM) or heptilidic acid (HA) (0.5 µM or 1µM) (A) or ML385 (1 µM) (B) followed by nigericin (10 µM) for 6 hours. **(C-D)** LDH (C) and IL-1ß (D) release from WT primary BMDMs treated with LPS for 2 hours, DMSO (vehicle) or DMF (25 µM) for 1 hour, HA or ML385 (1 µM) for 1 hour followed by nigericin (10 µM) or 1 hour. **(E-F)** Immunoblot analysis of GSDMD in cell lysates from WT BMDMs treated as in (B) with the indicated inhibitors. **(G-H)** QPCR (G) and immunoblot (H) analysis of *Nos2*/iNos in WT BMDMs treated with DMSO (vehicle) or HA (1 µM) for 1 hour and LPS for 3 (G) or 6 (H) hours. **(I)** QPCR analysis of *Hmox1* mRNA in WT BMDMs treated with DMSO (vehicle) or ML385 (1µM) for 3 hours. **(J-K)** LDH assay (J) and immunoblot analysis of GSDMD (K) in WT BMDMs transfected with control non-targeting siRNA or NRF2-specific siRNAs (50 nM) for 48 hours followed by treatment with LPS for 2 hours, DMSO (vehicle) or DMF (25 µM) and nigericin (10 µM) or 1 hour. A, B, E, F, H, K representative images from 3 independent experiments. C, D, G, I, K pooled data from 3 independent experiments. *, $P < 0.01$, ****, $P < 0.00001$ (Two-way ANOVA). Error bars show means ± SD (A, B) or SEM (C, D, G, I, J).

Figure S4

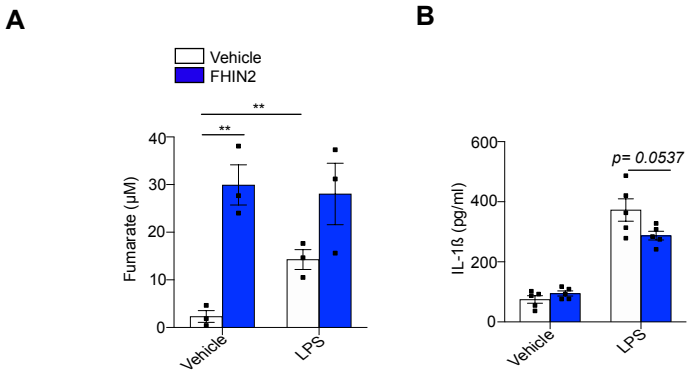

Fig. S4. Fumarate inhibits pyroptosis in vivo. (A-B) LC/MS Fumarate quantification in spleenocytes (A) and IL-1 ELISA analysis (B) in serum from WT C57/BL6 mice administered FHIN2 (50 mg/kg) by IP injection followed by LPS (10 mg/kg) by IP injection for 5 hours. Data points indicative of individual mice from one experiment. **, $P < 0.01$ (Two-way ANOVA). Error bars show means ± SEM.

Figure S5

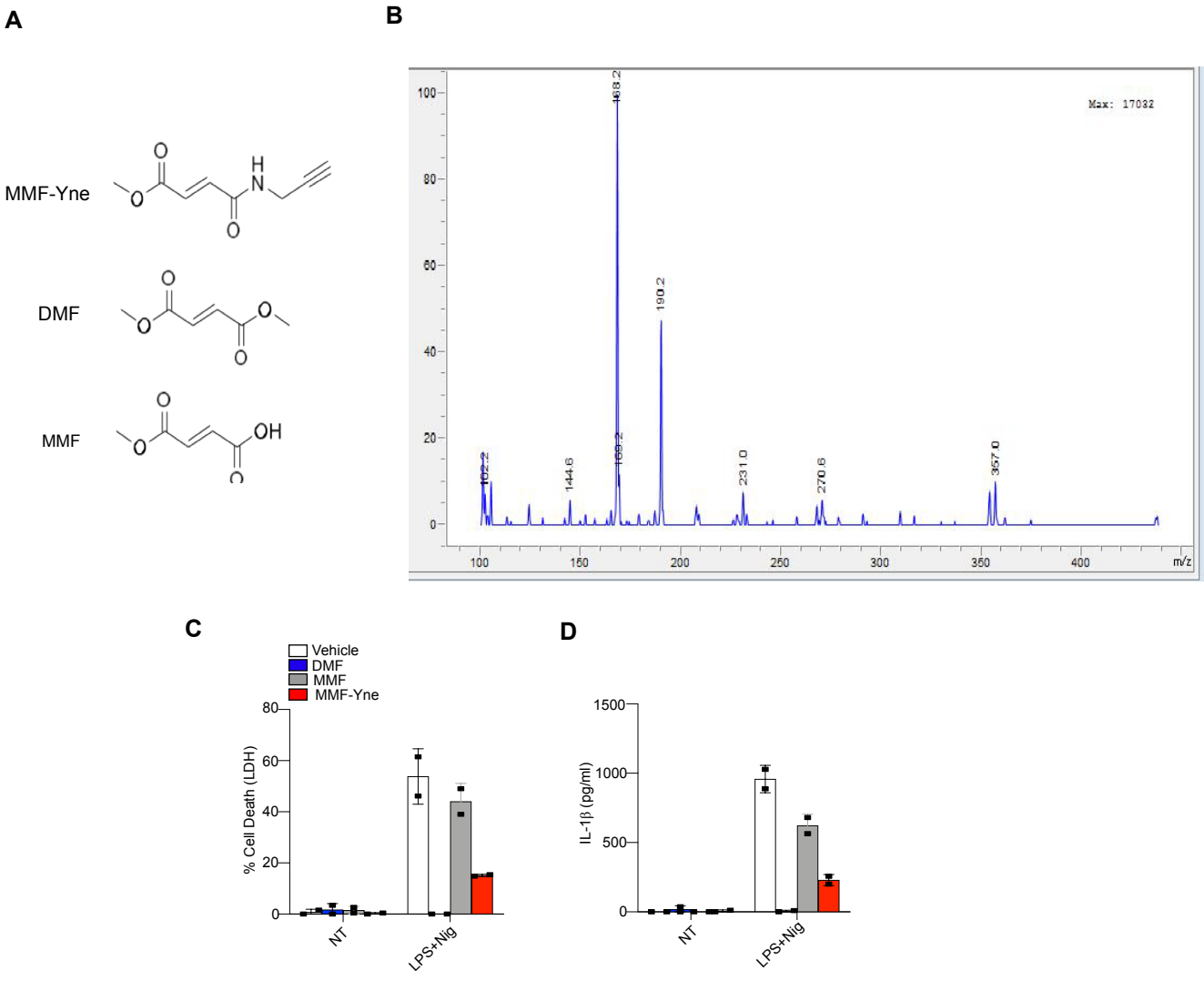

Fig. S5. Synthesis of MMF-Yne probe. (A) Structures of MMF-Alkyne, fumarate and MMF. **(B)** ESI-MS spectrum of MMF-Yne. **(C-D)** LDH (C) and IL-1β (D) release from WT BMDMs treated with LPS for 2 hours with DMSO (vehicle) or DMF (25 μM) for 1 hour, MMF (25 μM) or the MMF-Alkyne (25 μM) probe followed by treatment with nigericin (10 μM) for 1 hour. C, D pooled data from 2 independent experiments. Error bars show means ± SEM.

Figure S6

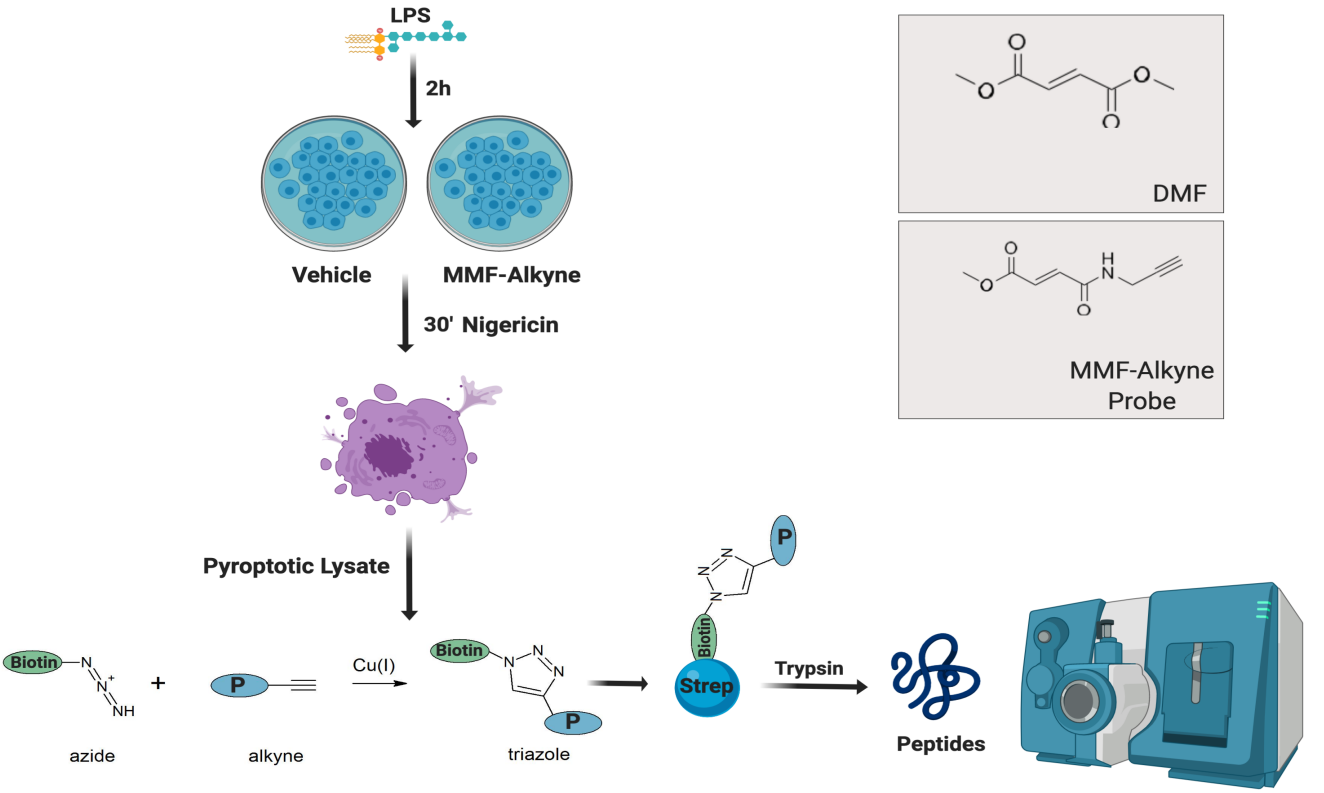

Fig. S6. Schematic of click-chemistry based proteomics. Schematic representation of MMF-Yne proteomics. Primary WT BMDMs were treated with LPS for 2hrs, MMF-Yne for 1 hour and nigericin (10 µM) for 1 hour. Lysates were subsequently Cu2+ clicked using a biotin-azide and streptavidin beads for pulldown of MMF-Yne interacting proteins. Streptavidin beads were digested using trypsin, reduced and alkylated and subjected to mass spec analysis.

Figure S7

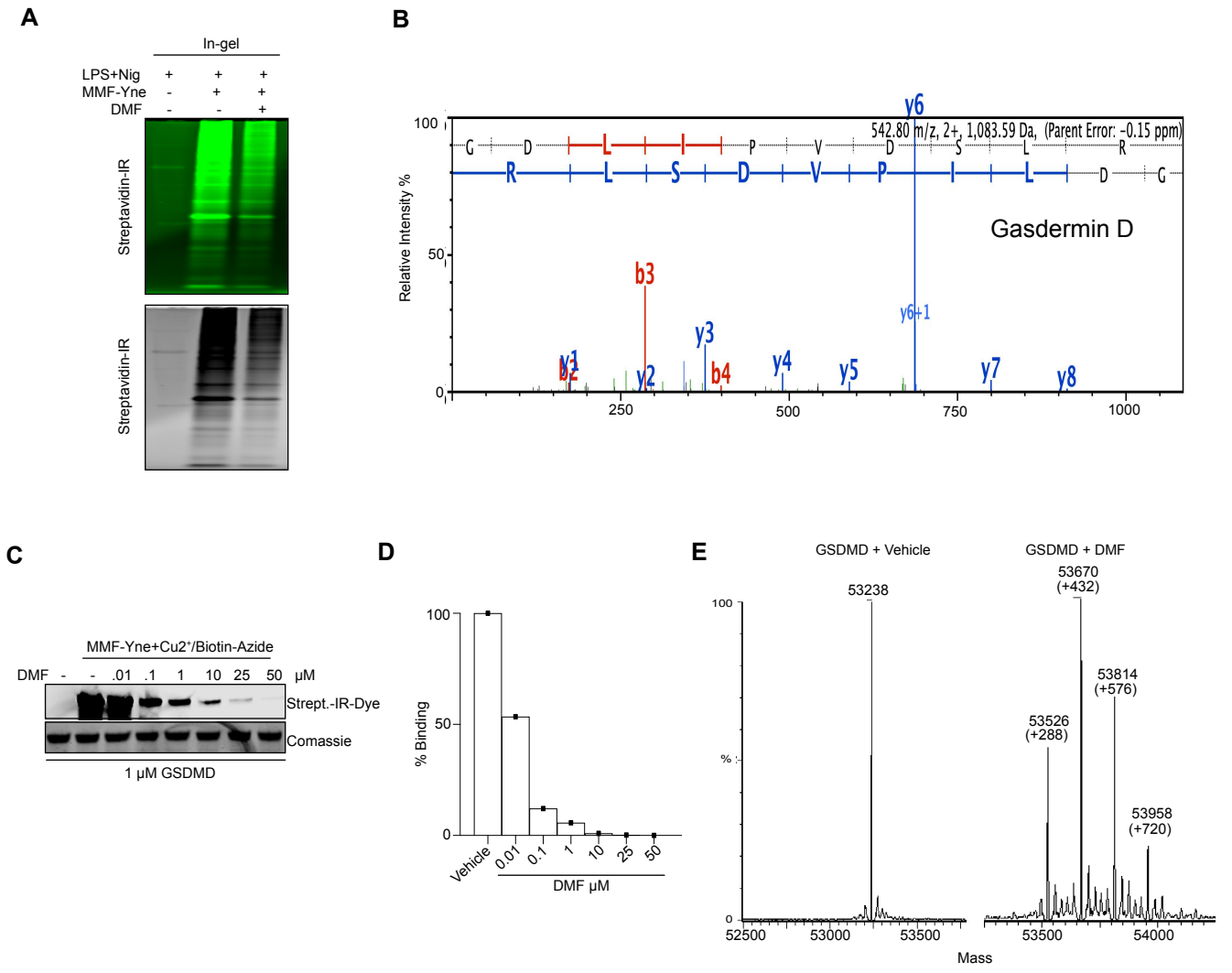

Fig. S7. Fumarate binds to GSDMD. (A) Immunoblot analysis of MMF-Yne bound proteins using a streptavidin-IR dye. **(B)** Representative MS spectra of GSDMD identified in streptavidin pulldowns subjected to mass spec. **(C-D)** Immunoblot analysis (C) and densitometry analysis (D) of streptavidin-IR dye detecting MMF-Yne labelled recombinant GSDMD incubated with the indicated concentrations of DMF and copper clicked using a biotin-azide. **(E)** Intact MS analysis of recombinant GSDMD (1 µM) incubated in a succination reaction with DMSO (vehicle) or DMF (25 µM) for 2 hours. A-E Representative images from 2 independent experiments.

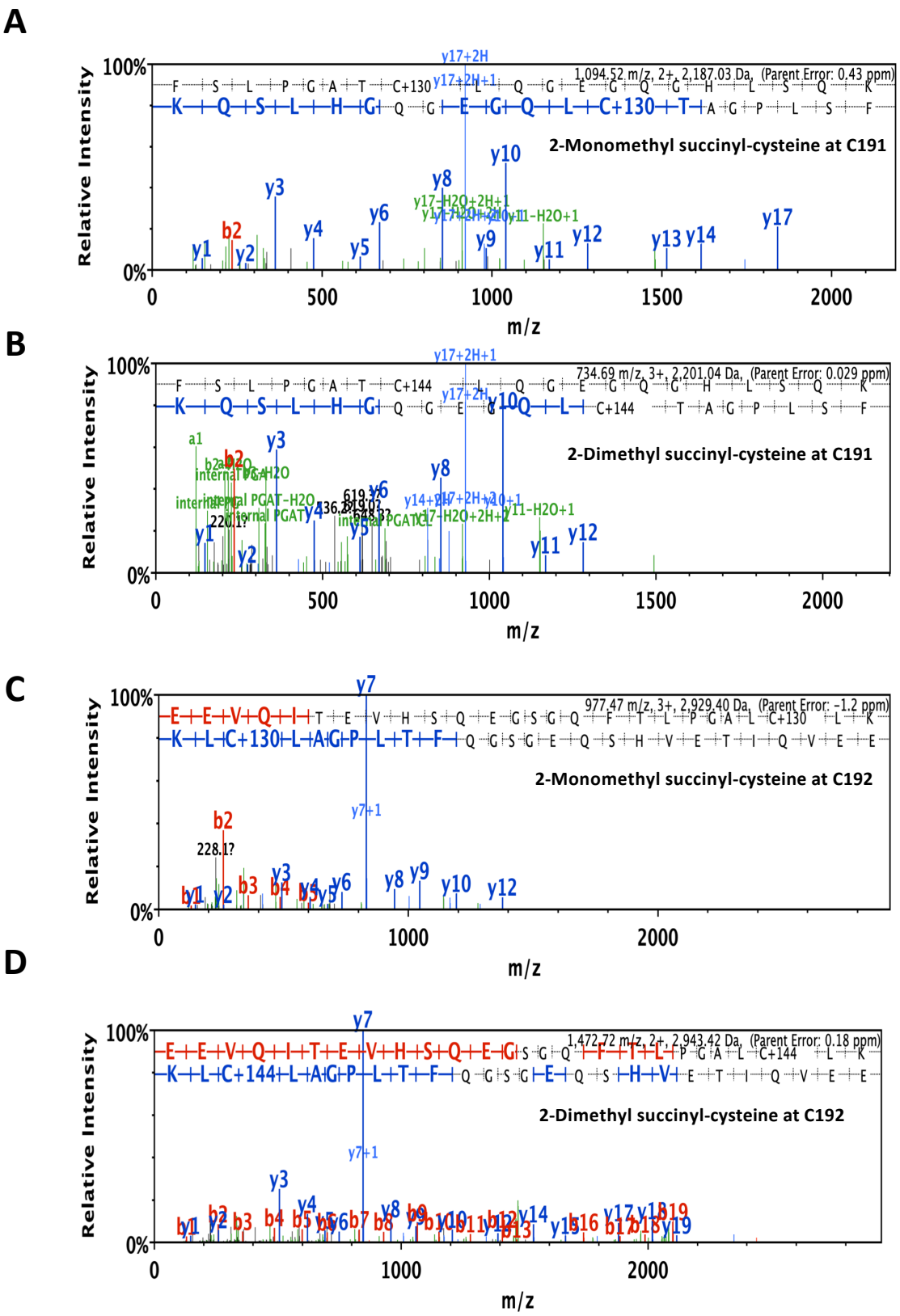

Fig. S8. In vitro succination of Human and Murine GSDMD (A-D) Representative MS spectra of 2-monomethyl succination (A, C) and 2-dimethylsuccination (B, D) of Human GSDMD (A, B) at Cys^{191} and Murine GSDMD (C, D) at Cys^{192}.

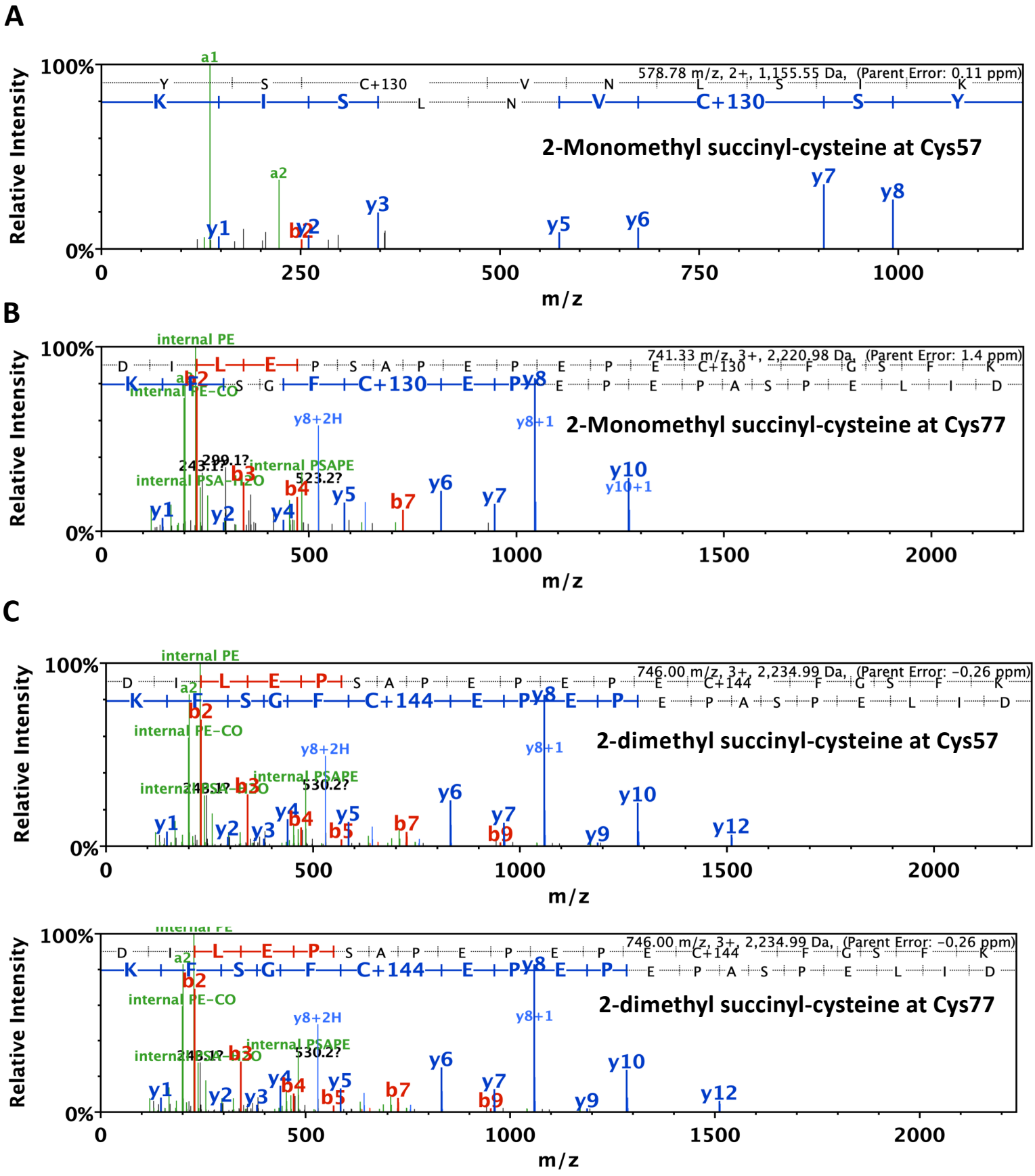

Fig. S9 Succination of endogenous gasdermin-d on Cys[57] and Cys[77]. (A-D) Representative MS spectra of 2-monomethyl succination (A-B) and 2-dimethylsuccination (C-D) of Cys[57] (A, C) and Cys[77] (B, D) GSDMD immunoprecipitated from WT BMDMs treated with Fumarate for 2 hours.

Figure S10

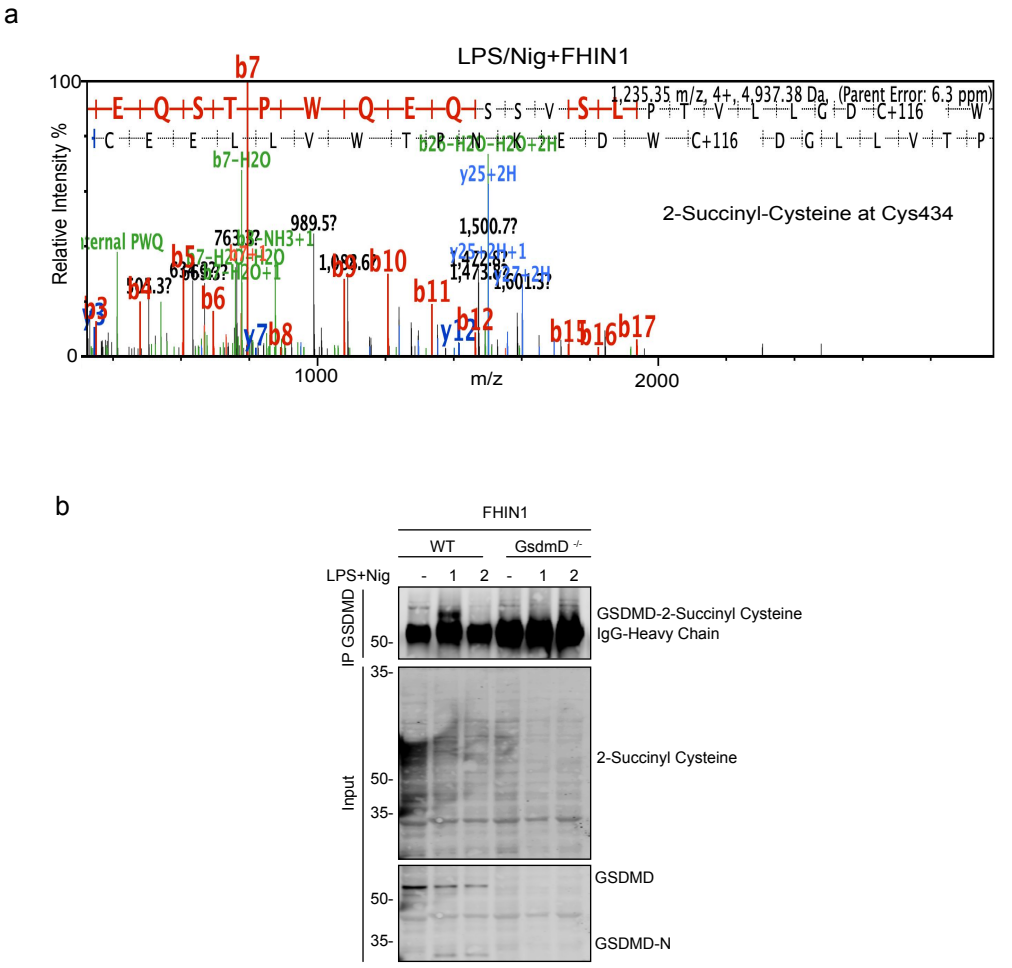

Fig. S10. Succination of GSDMD by endogenous fumarate (A) Representative MS spectra of 2-succinyl succination on Cys^{434} of GSDMD immunoprecipitated from WT BMDMs treated with FHIN1 (50 μM) for 1 hour, LPS for 2 hours and nigericin (10 μM) for the indicated times. **(B)** Immunoblot of 2-succinyl-cysteine and GSDMD in immunoprecipitates (IP) and lysates (input) from WT and *Gsdmd*$^{-/-}$ BMDMs. Representative experiments.

Figure S11

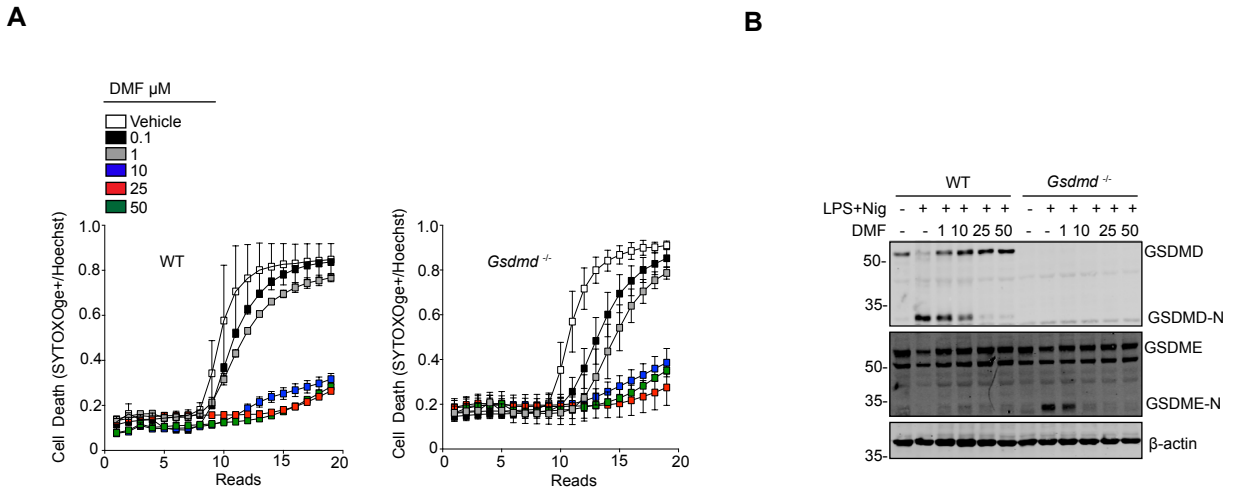

Fig. S11. Fumarate inhibits GSDMD and GSDME comparably. (A) Kinetic cell death data of WT (left-panel) and *Gsdmd*$^{-/-}$ (right-panel) primary BMDMs with LPS for 2 hours, DMSO (vehicle) or DMF (0-50 µM) followed by nigericin (10 µM) for 6 hours. **(B)** Immunoblot analysis of GSDMD, GSDME and -actin in cell lysates from WT and *Gsdmd*$^{-/-}$ BMDMs treated as in (A). A-B represenatative of 3 indpendent experiments.

Figure S12

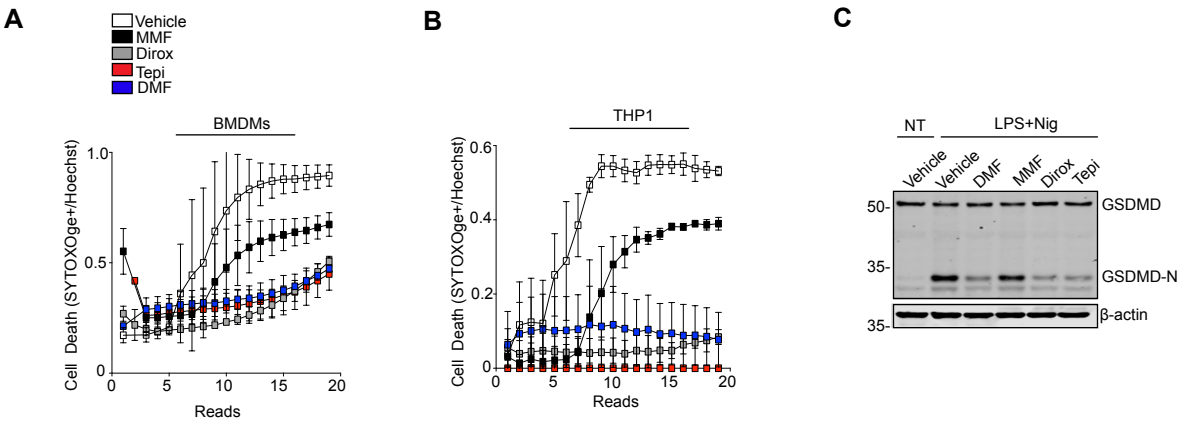

Fig. S12. Fumarate analogues inhibit pyroptosis (A) Kinetic cell death data of WT primary BMDMs (A) and THP1 cells (B) stained with SytoxOge and Hoechst following treatment with LPS for 2hr, DMSO (Vehicle), DMF, MMF, Diroximel Fumarate (Dirox) or Tepilamide (Tepi), for 1 hour and nigericin for the indicated time course. **(C)** Immunoblot analysis of GSDMD cell lysates from WT BMDMs treated as in (A) with the indicated fumarate analogues (25 μM). A-C are representative of 3 independent experiments.

Figure S13

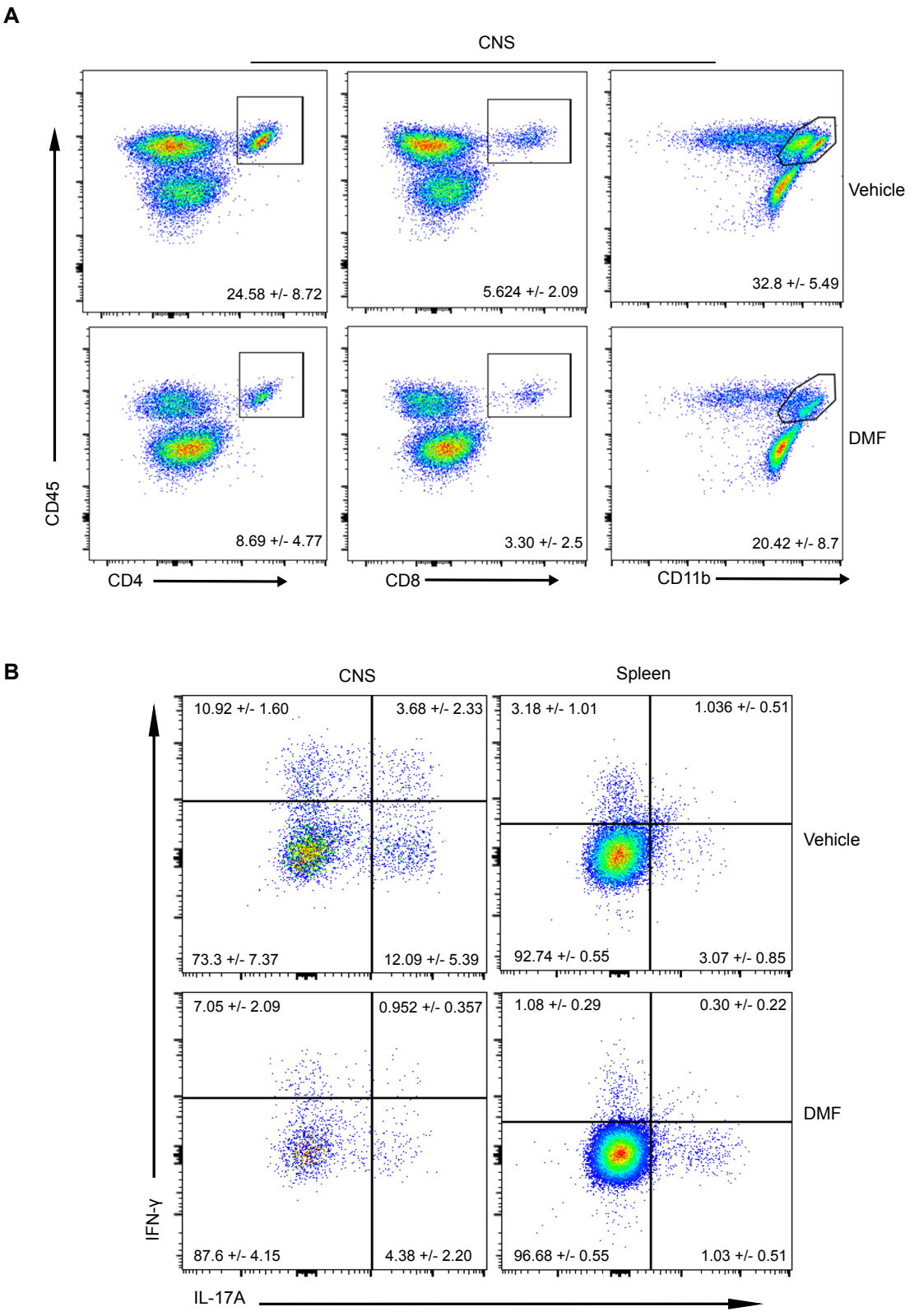

Fig. S13. Representative flow cytometry plots from Figure 4.

Figure S14

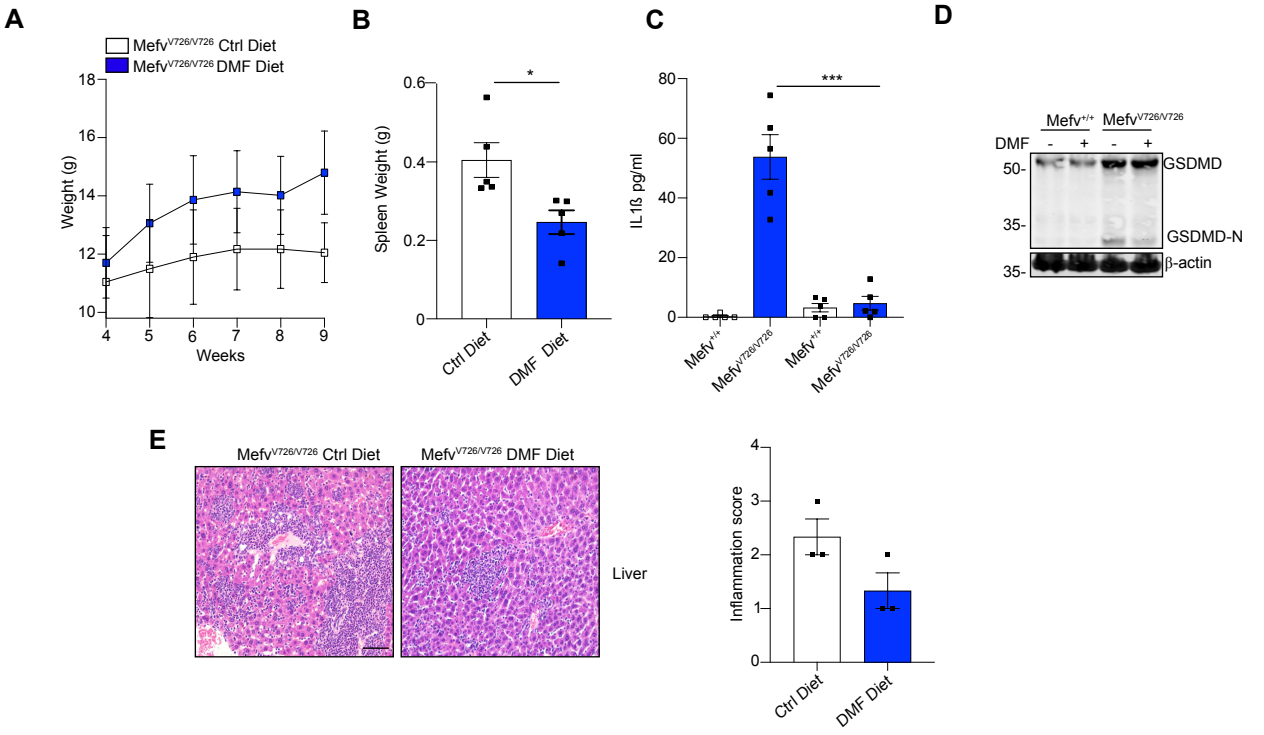

Fig. S14. Fumarate alleviates FMF. (A-E) Weight gain (A), spleen weight (B), ELISA of serum IL-β and immunoblot of spleen GSDMD (D) liver H&E (E) from Mefv$^{726/726}$ receiving vehicle diet or a diet containing DMF (100 mg/kg/day) for 6 weeks. Scale bar 100 µm. Data points indicative of individual mice from two independent experiments. *, P<0.05 ***, P < 0.001 (t-test or Two-way ANOVA). Error bars show means ± SEM.

Figure S15

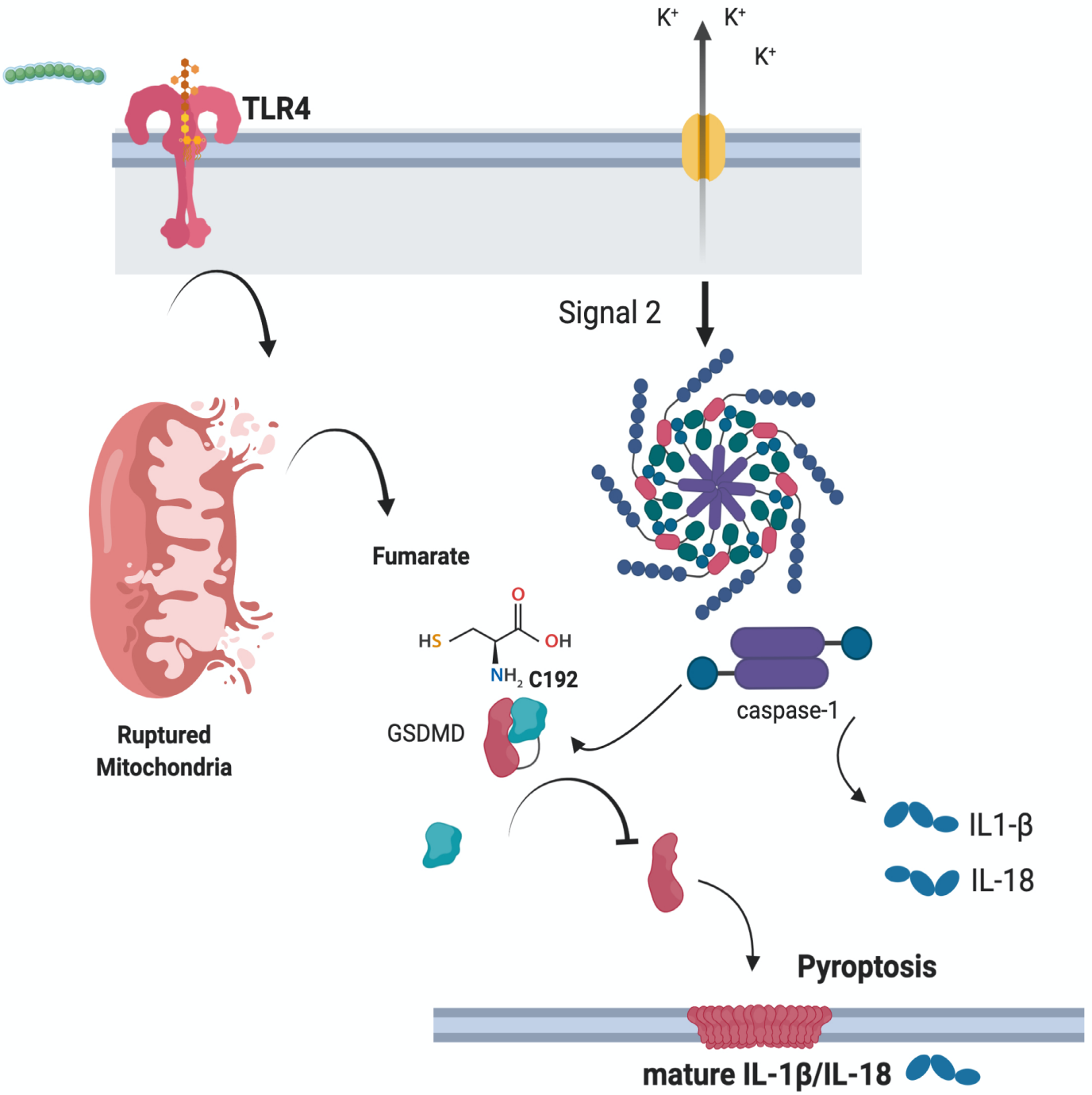

Fig. S15. Proposed mechanism of fumarate mediated regulation of Pyroptosis. Mitochondrial membrane rupture during pyroptosis results in accumulation of fumarate in the cytosol. Fumarate released during inflammasome activation results in the succination of Cys^{192} in gasdermin-d. Succination of GSDMD results in impaired GSDMD oligomerization and pyroptosis.

Table S1

Species	h.GSDMD		m.GSDMD		h.GSDME	
	MMF	DMF	MMF	DMF	MMF	DMF
	Cys56	Cys56	Cys39	Cys39	Cys45	Cys45
	Cys191	Cys191	Cys57	Cys57	Cys156	Cys156
	Cys268	Cys268	Cys77	Cys77	Cys168	Cys180
	Cys309	Cys309	Cys192	Cys122	Cys180	Cys235
	Cys467	Cys467	Cys265	Cys192	Cys235	Cys371
			Cys299	Cys265	Cys371	Cys408
			Cys434	Cys299	Cys417	Cys489
			Cys487	Cys434	Cys489	
				Cys448		
				Cys489		

Table S1. In vitro cysteine succination sites in GSDMD and GSDME

Table S2

Cysteine	Assay	Modified Peptide sequence
Human Cys191	In vitro	KISGGAAVDSSASMNVC(2DSC)ILRV
Human Cys191	In vitro	RFSLPGATC(2MSC)LQEGQGHLSQKK
Murine Cys192	In vitro	ISGGAAVSDSSSASMNVC(2DSC)ILRV
Murine Cys192	In vitro	EEVQITEVHSQEGSGQFTLPGALC(2MSC)LKG
Murine Cys192	Primary BMDMs	KEEVQITEVHSQEGSGQFTLPGAL(2DSC)LKG
Murine Cys192	Primary BMDMs	KEEVQITEVHSQEGSGQFTLPGAL(2MSC)LKG

Table S2. Representative peptides of Cys192 modified by 2-dimethyl succination (2DSC) and 2-monomethylsuccination (2MSC)

Table S3

Patient #	Gender	Age	BMI	Diagnosis	MS Type	EDSS	SDMT	25Ft-walk	Peg Test	Tecfidera
21	Male	62	26.18	1985	RRPMS	6.5	54	9.09	25	-
22	Female	50	31.68	1992	RPMS	6.5	38	25.32	36.41	-
93	Female	58	21.28	N/A	SPMS	6.5	57	20.6	13.2	-
321	Male	73	24.64	1989	PMS	6.5	50	8.6	17.5	-
137	Female	53	22.25	2004	SPMS	6.5	43	6.8	10.5	-
324	Female	52	21.22	1994	SPMS	5	32	8	15.35	-
326	Male	65	31.71	N/A	SPMS	8	22	N/A	38.7	-
328	Female	61	39.74	N/A	SPMS	8.5	N/A	N/A	N/A	-
132	Female	51	19.97	1991	SPMS	6.5	37	13.13	78	-
337	Female	41	21.1	2009	RR	1.5	65	3.3	10.7	+
253	Female	58	23.53	1997	SPMS	4.5	21	17.53	17.53	+
301	Male	68	27.28	2005	PMS	7	31	22.1	22.1	+
224	Female	73	26.26	1985	PMS	6	21	25.5	25.5	+
320	Female	67	30.36	1987	SPMS	3.5	33	10.3	10.3	+
218	Female	53	18.36	2018	SPMS	1.5	58	10.22	10.22	+
253	Female	59	23.53	1996	SPMS	4.5	21	17.53	17.53	+
342	Female	58	30.07	1984	SPMS	1	50	12.59	12.59	+
257	Male	44	36.1	2018	RR	3.5	43	5.9	19.8	+

Table S3. Clinical evaluation and patient information related to Figure 4I-K. Expanded disability status scale (EDSS), Symbol digit modalities test (SDMT), times 25-foot walk test (25Ft-walk), 9-hole peg test (Peg Test), body mass index (BMI), Not Available (N/A). Refractory relapsing PMS, (RRPMS), progressive MS (PMS), secondary progressive MS (SPMS), relapsing remitting (RR).

Table S4

Patient #	Gender	Age	MS Type	EDSS	PMI (h)
MS-18	Male	45	SPMS	7	3
MS-25	Male	56	SPMS	9.5	3
MS-147	Female	50	RR	3	7

Table S4. Clinical evaluation patient information related to Figure 4L. Expanded disability status scale (EDSS), post-mortem interval hours (PMI). Secondary progressive MS (SPMS). Relapsing remitting (RR).

References and Notes

1. J. Shi, Y. Zhao, K. Wang, X. Shi, Y. Wang, H. Huang, Y. Zhuang, T. Cai, F. Wang, F. Shao, Cleavage of GSDMD by inflammatory caspases determines pyroptotic cell death. *Nature* **526**, 660–665 (2015). doi:10.1038/nature15514 Medline

2. N. Kayagaki, I. B. Stowe, B. L. Lee, K. O'Rourke, K. Anderson, S. Warming, T. Cuellar, B. Haley, M. Roose-Girma, Q. T. Phung, P. S. Liu, J. R. Lill, H. Li, J. Wu, S. Kummerfeld, J. Zhang, W. P. Lee, S. J. Snipas, G. S. Salvesen, L. X. Morris, L. Fitzgerald, Y. Zhang, E. M. Bertram, C. C. Goodnow, V. M. Dixit, Caspase-11 cleaves gasdermin D for non-canonical inflammasome signalling. *Nature* **526**, 666–671 (2015). doi:10.1038/nature15541 Medline

3. E. L. Mills, D. G. Ryan, H. A. Prag, D. Dikovskaya, D. Menon, Z. Zaslona, M. P. Jedrychowski, A. S. H. Costa, M. Higgins, E. Hams, J. Szpyt, M. C. Runtsch, M. S. King, J. F. McGouran, R. Fischer, B. M. Kessler, A. F. McGettrick, M. M. Hughes, R. G. Carroll, L. M. Booty, E. V. Knatko, P. J. Meakin, M. L. J. Ashford, L. K. Modis, G. Brunori, D. C. Sévin, P. G. Fallon, S. T. Caldwell, E. R. S. Kunji, E. T. Chouchani, C. Frezza, A. T. Dinkova-Kostova, R. C. Hartley, M. P. Murphy, L. A. O'Neill, Itaconate is an anti-inflammatory metabolite that activates Nrf2 via alkylation of KEAP1. *Nature* **556**, 113–117 (2018). doi:10.1038/nature25986 Medline

4. S.-T. Liao, C. Han, D.-Q. Xu, X.-W. Fu, J.-S. Wang, L.-Y. Kong, 4-Octyl itaconate inhibits aerobic glycolysis by targeting GAPDH to exert anti-inflammatory effects. *Nat. Commun.* **10**, 5091 (2019). doi:10.1038/s41467-019-13078-5 Medline

5. V. Lampropoulou, A. Sergushichev, M. Bambouskova, S. Nair, E. E. Vincent, E. Loginicheva, L. Cervantes-Barragan, X. Ma, S. C.-C. Huang, T. Griss, C. J. Weinheimer, S. Khader, G. J. Randolph, E. J. Pearce, R. G. Jones, A. Diwan, M. S. Diamond, M. N. Artyomov, Itaconate Links Inhibition of Succinate Dehydrogenase with Macrophage Metabolic Remodeling and Regulation of Inflammation. *Cell Metab.* **24**, 158–166 (2016). doi:10.1016/j.cmet.2016.06.004 Medline

6. M. Bambouskova, L. Gorvel, V. Lampropoulou, A. Sergushichev, E. Loginicheva, K. Johnson, D. Korenfeld, M. E. Mathyer, H. Kim, L.-H. Huang, D. Duncan, H. Bregman, A. Keskin, A. Santeford, R. S. Apte, R. Sehgal, B. Johnson, G. K. Amarasinghe, M. P. Soares, T. Satoh, S. Akira, T. Hai, C. de Guzman Strong, K. Auclair, T. P. Roddy, S. A. Biller, M. Jovanovic, E. Klechevsky, K. M. Stewart, G. J. Randolph, M. N. Artyomov, Electrophilic properties of itaconate and derivatives regulate the IκBζ-ATF3 inflammatory axis. *Nature* **556**, 501–504 (2018). doi:10.1038/s41586-018-0052-z Medline

7. G. M. Tannahill, A. M. Curtis, J. Adamik, E. M. Palsson-McDermott, A. F. McGettrick, G. Goel, C. Frezza, N. J. Bernard, B. Kelly, N. H. Foley, L. Zheng, A. Gardet, Z. Tong, S. S. Jany, S. C. Corr, M. Haneklaus, B. E. Caffrey, K. Pierce, S. Walmsley, F. C. Beasley, E. Cummins, V. Nizet, M. Whyte, C. T. Taylor, H. Lin, S. L. Masters, E. Gottlieb, V. P. Kelly, C. Clish, P. E. Auron, R. J. Xavier, L. A. J. O'Neill, Succinate is an inflammatory signal that induces IL-1β through HIF-1α. *Nature* **496**, 238–242 (2013). doi:10.1038/nature11986 Medline

8. J. S. Muhammad, M. N. Jayakumar, N. M. Elemam, T. Venkatachalam, T. K. Raju, R. A. Hamoudi, A. A. Maghazachi, Gasdermin D Hypermethylation Inhibits Pyroptosis And LPS-Induced IL-1β Release From NK92 Cells. *ImmunoTargets Ther.* **8**, 29–41 (2019). doi:10.2147/ITT.S219867 Medline

9. M. Blatnik, N. Frizzell, S. R. Thorpe, J. W. Baynes, Inactivation of glyceraldehyde-3-phosphate dehydrogenase by fumarate in diabetes: Formation of S-(2-succinyl)cysteine, a novel chemical modification of protein and possible biomarker of mitochondrial stress. *Diabetes* **57**, 41–49 (2008). doi:10.2337/db07-0838 Medline

10. M. D. Kornberg, P. Bhargava, P. M. Kim, V. Putluri, A. M. Snowman, N. Putluri, P. A. Calabresi, S. H. Snyder, Dimethyl fumarate targets GAPDH and aerobic glycolysis to modulate immunity. *Science* **360**, 449–453 (2018). doi:10.1126/science.aan4665 Medline

11. A. Singh, S. Venkannagari, K. H. Oh, Y.-Q. Zhang, J. M. Rohde, L. Liu, S. Nimmagadda, K. Sudini, K. R. Brimacombe, S. Gajghate, J. Ma, A. Wang, X. Xu, S. A. Shahane, M. Xia, J. Woo, G. A. Mensah, Z. Wang, M. Ferrer, E. Gabrielson, Z. Li, F. Rastinejad, M. Shen, M. B. Boxer, S. Biswal, Small Molecule Inhibitor of NRF2 Selectively Intervenes Therapeutic Resistance in KEAP1-Deficient NSCLC Tumors. *ACS Chem. Biol.* **11**, 3214–3225 (2016). doi:10.1021/acschembio.6b00651 Medline

12. M. Kato, K. Sakai, A. Endo, Koningic acid (heptelidic acid) inhibition of glyceraldehyde-3-phosphate dehydrogenases from various sources. *Biochim. Biophys. Acta* **1120**, 113–116 (1992). doi:10.1016/0167-4838(92)90431-C Medline

13. R. A. Kulkarni, D. W. Bak, D. Wei, S. E. Bergholtz, C. A. Briney, J. H. Shrimp, A. Alpsoy, A. L. Thorpe, A. E. Bavari, D. R. Crooks, M. Levy, L. Florens, M. P. Washburn, N. Frizzell, E. C. Dykhuizen, E. Weerapana, W. M. Linehan, J. L. Meier, A chemoproteomic portrait of the oncometabolite fumarate. *Nat. Chem. Biol.* **15**, 391–400 (2019). doi:10.1038/s41589-018-0217-y Medline

14. X. Liu, Z. Zhang, J. Ruan, Y. Pan, V. G. Magupalli, H. Wu, J. Lieberman, Inflammasome-activated gasdermin D causes pyroptosis by forming membrane pores. *Nature* **535**, 153–158 (2016). doi:10.1038/nature18629 Medline

15. J. J. Hu, X. Liu, S. Xia, Z. Zhang, Y. Zhang, J. Zhao, J. Ruan, X. Luo, X. Lou, Y. Bai, J. Wang, L. R. Hollingsworth, V. G. Magupalli, L. Zhao, H. R. Luo, J. Kim, J. Lieberman, H. Wu, FDA-approved disulfiram inhibits pyroptosis by blocking gasdermin D pore formation. *Nat. Immunol.* **21**, 736–745 (2020). doi:10.1038/s41590-020-0669-6 Medline

16. C. Rogers, D. A. Erkes, A. Nardone, A. E. Aplin, T. Fernandes-Alnemri, E. S. Alnemri, Gasdermin pores permeabilize mitochondria to augment caspase-3 activation during apoptosis and inflammasome activation. *Nat. Commun.* **10**, 1689 (2019). doi:10.1038/s41467-019-09397-2 Medline

17. B. A. McKenzie, M. K. Mamik, L. B. Saito, R. Boghozian, M. C. Monaco, E. O. Major, J.-Q. Lu, W. G. Branton, C. Power, Caspase-1 inhibition prevents glial inflammasome activation and pyroptosis in models of multiple sclerosis. *Proc. Natl. Acad. Sci. U.S.A.* **115**, E6065–E6074 (2018). doi:10.1073/pnas.1722041115 Medline

18. S. Li, Y. Wu, D. Yang, C. Wu, C. Ma, X. Liu, P. N. Moynagh, B. Wang, G. Hu, S. Yang, Gasdermin D in peripheral myeloid cells drives neuroinflammation in experimental

autoimmune encephalomyelitis. *J. Exp. Med.* **216**, 2562–2581 (2019). doi:10.1084/jem.20190377 Medline

19. A. Kanneganti, R. K. S. Malireddi, P. H. V. Saavedra, L. Vande Walle, H. Van Gorp, H. Kambara, H. Tillman, P. Vogel, H. R. Luo, R. J. Xavier, H. Chi, M. Lamkanfi, GSDMD is critical for autoinflammatory pathology in a mouse model of Familial Mediterranean Fever. *J. Exp. Med.* **215**, 1519–1529 (2018). doi:10.1084/jem.20172060 Medline

20. J. K. Rathkey, J. Zhao, Z. Liu, Y. Chen, J. Yang, H. C. Kondolf, B. L. Benson, S. M. Chirieleison, A. Y. Huang, G. R. Dubyak, T. S. Xiao, X. Li, D. W. Abbott, Chemical disruption of the pyroptotic pore-forming protein gasdermin D inhibits inflammatory cell death and sepsis. *Sci. Immunol.* **3**, eaat2738 (2018). doi:10.1126/sciimmunol.aat2738 Medline

21. G. Sollberger, A. Choidas, G. L. Burn, P. Habenberger, R. Di Lucrezia, S. Kordes, S. Menninger, J. Eickhoff, P. Nussbaumer, B. Klebl, R. Krüger, A. Herzig, A. Zychlinsky, Gasdermin D plays a vital role in the generation of neutrophil extracellular traps. *Sci. Immunol.* **3**, eaar6689 (2018). doi:10.1126/sciimmunol.aar6689 Medline

22. P. Orning, D. Weng, K. Starheim, D. Ratner, Z. Best, B. Lee, A. Brooks, S. Xia, H. Wu, M. A. Kelliher, S. B. Berger, P. J. Gough, J. Bertin, M. M. Proulx, J. D. Goguen, N. Kayagaki, K. A. Fitzgerald, E. Lien, Pathogen blockade of TAK1 triggers caspase-8-dependent cleavage of gasdermin D and cell death. *Science* **362**, 1064–1069 (2018). doi:10.1126/science.aau2818 Medline

23. J. J. Chae, Y.-H. Cho, G.-S. Lee, J. Cheng, P. P. Liu, L. Feigenbaum, S. I. Katz, D. L. Kastner, Gain-of-function Pyrin mutations induce NLRP3 protein-independent interleukin-1β activation and severe autoinflammation in mice. *Immunity* **34**, 755–768 (2011). doi:10.1016/j.immuni.2011.02.020 Medline

24. R. Dutta, K. R. Mahajan, K. Nakamura, D. Ontaneda, J. Chen, C. Volsko, J. Dudman, E. Christie, J. Dunham, R. J. Fox, B. D. Trapp, Comprehensive Autopsy Program for Individuals with Multiple Sclerosis. *J. Vis. Exp.* **149**, e59511 (2019). doi:10.3791/59511 Medline